Supplemental Information
Mean-Independent Noise Control via Intermediate States

Christopher Rackauckas, Thomas Schilling, and Qing Nie

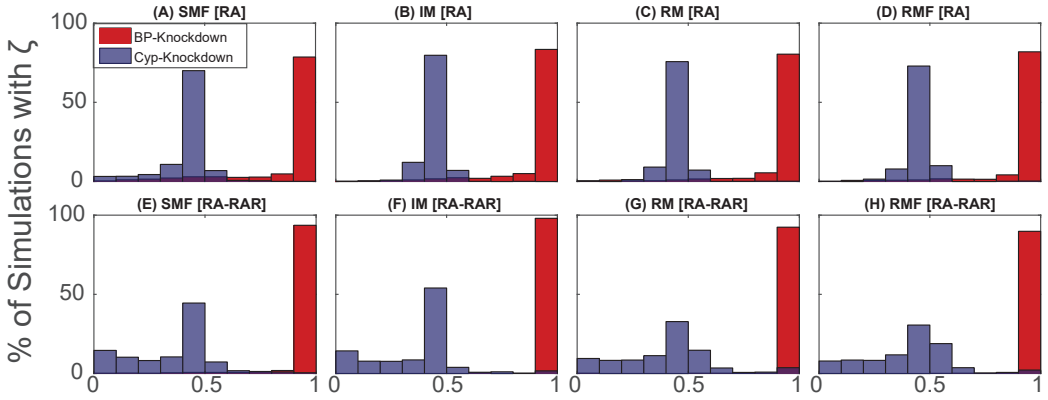

Figure 1: Mean and variance knockdown distributions with multiplicative noise. (A)-(H) Histograms depicting the ζ distribution due to multiplicative noise. The models were solved using the Euler-Maruyama method on the timespan of $t = [0, 200]$, and re-solved with the associated parameter reduced by 90%. The value ζ was calculated from these two series, and this was repeated 10,000 times. More details outlining the experiment are found in the STAR Methods. Figures (A)-(D) correspond to the ζ's calculated for [RA] on the respective models. Figures (E)-(H) correspond to the ζ's calculated for [RA-RAR] on the models the models respectively.

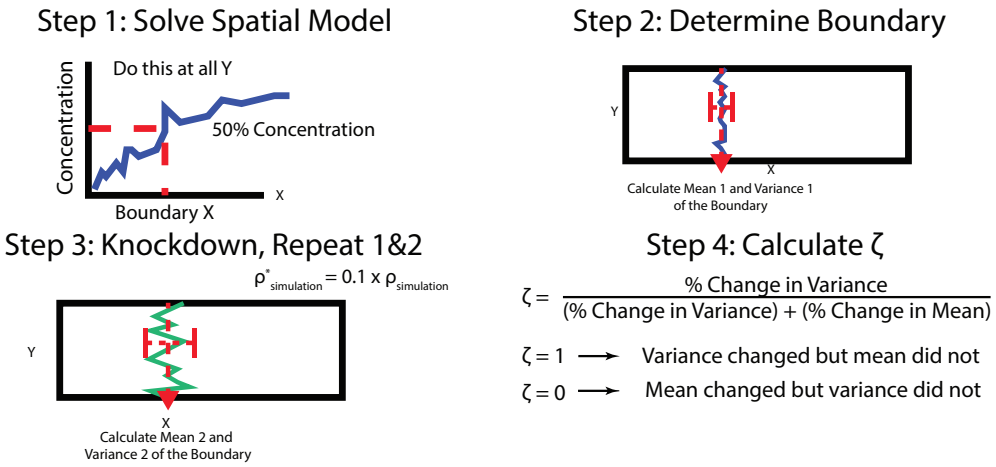

Figure 2: Diagram of Spatial Experiment. A diagram of the numerical scheme for the ζ histogram experiments for spatial location vs threshold sharpness. The SPDE model is solved and the 50% concentration point at each location along the x-axis is found. Then the mean and the variance of these x locations are saved. This process is then repeated with reduced binding protein and the resulting mean and variance values are compared with the previous to get a value for ζ.

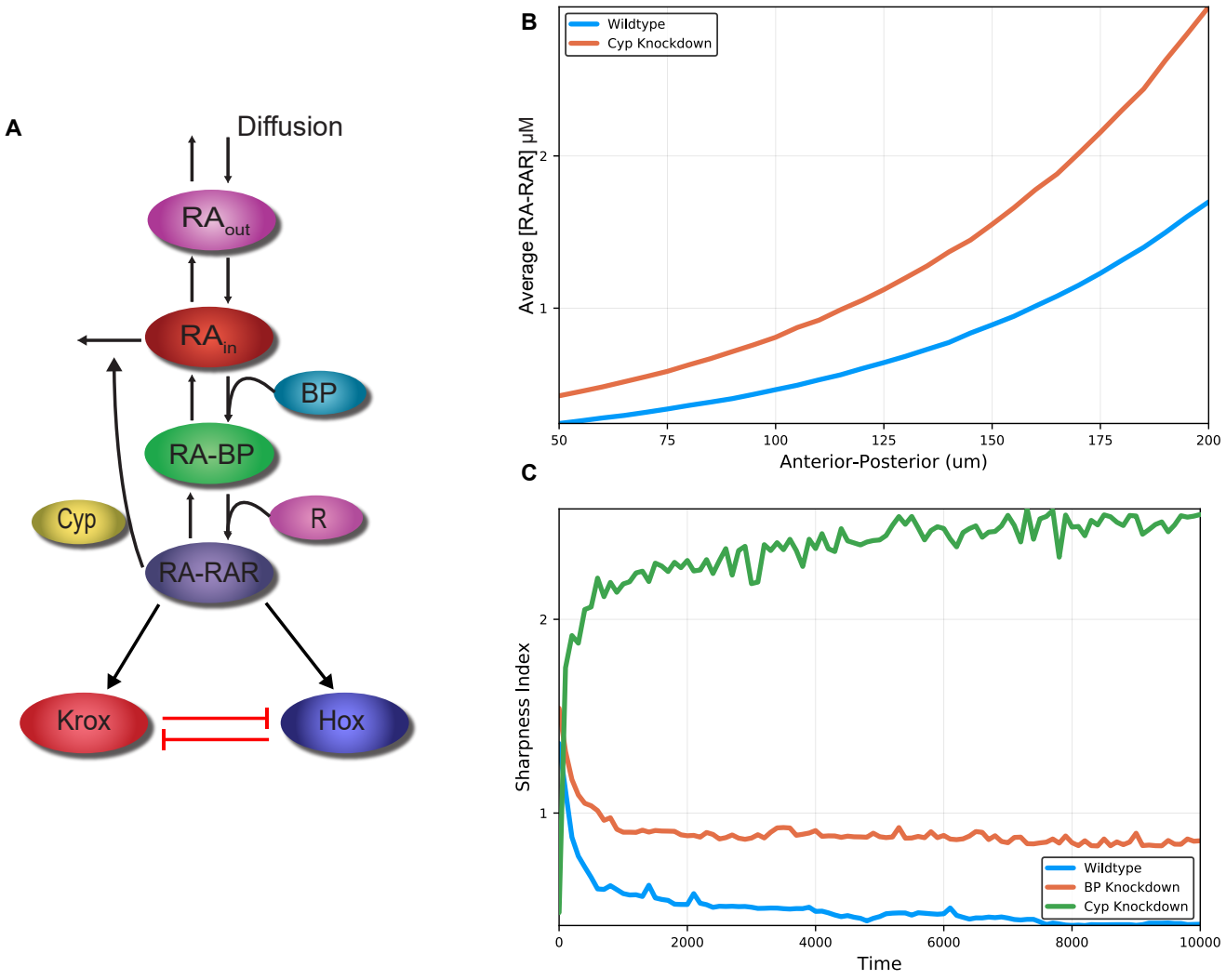

Figure 3: Boundary sharpening disruption extended figures. **(A)** Diagram of the extended RA model with downstream Hox-Krox signaling. Shown is the signaling diagram for the retinoic acid model starting with the diffusive RA_{out} which enters the cell to become RA_{in} and binds to BP to become $RA-BP$, which then binds to RAR produce $RA-RAR$. This $RA-RAR$ produces Cyp which deactivates (and thus degrades) the intercellular RA_{in}. Additionally, $RA-RAR$ acts as a signal to the downstream Hox and $Krox$ which are mutually antagonistic. **(B)** Mean shift of the RAR signal due to cyp knockdown. For the wildtype and Cyp26 setups in the extended RA model with Hox-Krox signaling, the mean of the [RA-RAR] gradient was calculated between each of the 10 runs at the ending timepoint. **(C)** Sharpness Index. The y-axis corresponds to the sharpness index defined in (Zhang et al., 2012). The x-axis shows time in terms of hpf. Each condition was ran 10 times and the results were averaged.

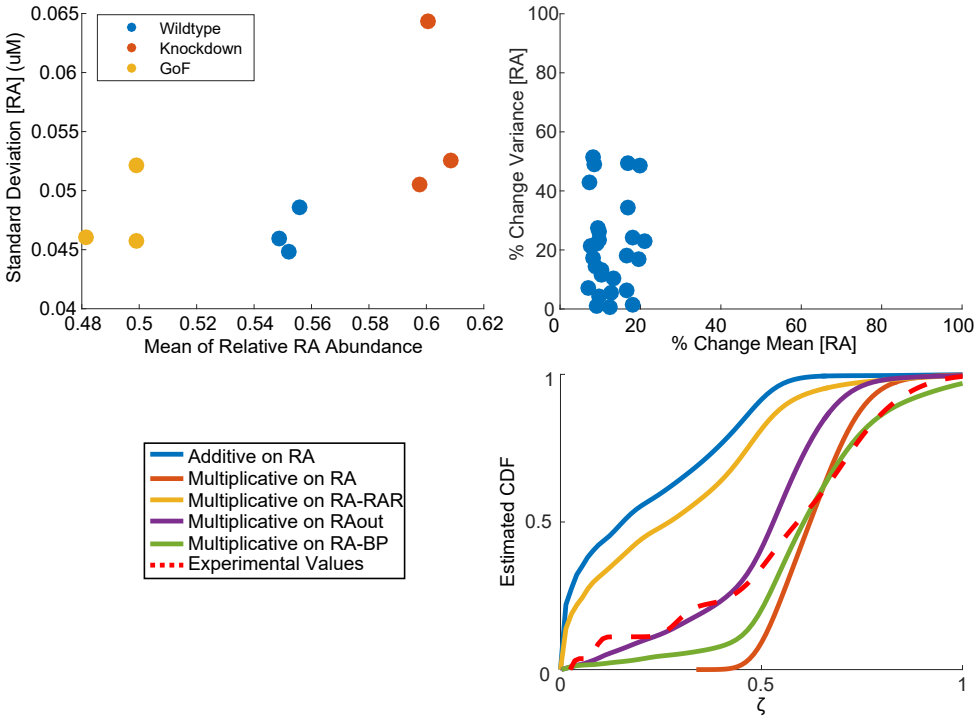

Figure 4: Characterization of ζ due to previous data. **(A)** Scatter plot of the data points from (Sosnik et al., 2016). **(B)** Pairwise Differences. The percent change in mean and variance was calculated pairwise between each pair of higher and lower data point. A scatter plot of the results is shown. **(C)** Estimated CDF. Depiction of the commutative probability distribution for ζ according to the parameter search scheme from the parameter search scheme on RMF. The simulations which produced these distributions is discussed in the STAR Methods. Shown are the kernel density estimates from the ζ values from the stochastic simulations. The different colored lines show the distributions for different noise types. The red line depict experimental CDF for ζ computed using the pairwise data points.

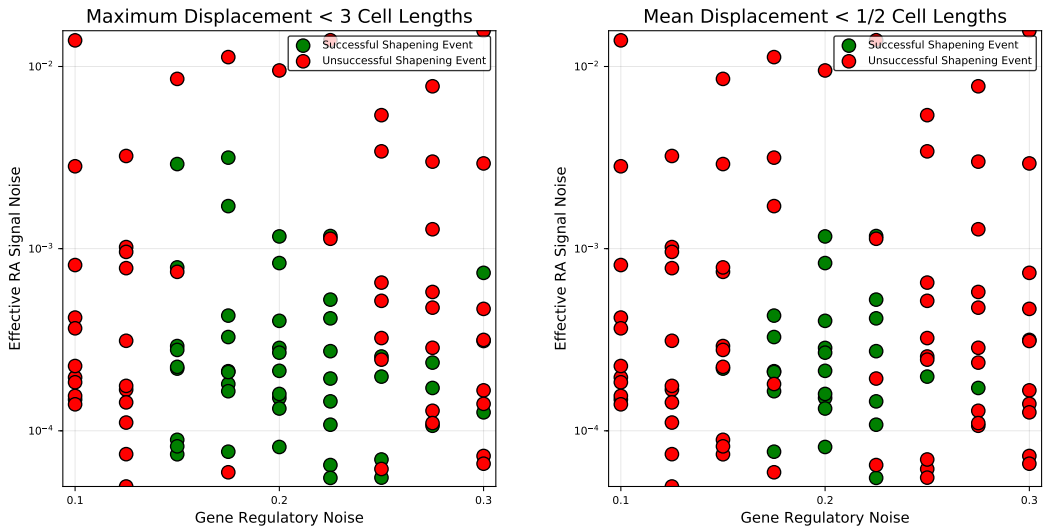

Figure 5: Additional characterization of successful sharpening via other measures. Binding protein production taken as 5, 15, . . . , 105 and Hox-Krox regulatory noise was taken as 0.1, 0.125, . . . , 0.3 and each pairing in the grid was solved once. The effective RA noise was calculated according to the measure from the STAR Methods section. In **(A)** a successful sharpening event was characterized by having the maximum displacement between Hox and Krox dominated cells of less than 3 cell lengths. In **(B)** a successful sharpening event was characterized by having the mean displacement betewen Hox and Krox dominated cells as less than $\frac{1}{2}$ of a cell length.